Cellular/Molecular

$G\beta_3$ Is Required for Normal Light ON Responses and Synaptic Maintenance

Anuradha Dhingra,[1] Hariharasubramanian Ramakrishnan,[1] Adam Neinstein,[1] Marie E. Fina,[1] Ying Xu,[4] Jian Li,[2] Daniel C. Chung,[3] Arkady Lyubarsky,[3] and Noga Vardi[1]

Departments of [1]Neuroscience, [2]Neurology, and [3]Ophthalmology, University of Pennsylvania, Philadelphia, Pennsylvania 19104, and [4]Joint Laboratory for Brain Function and Health, Jinan University and the University of Hong Kong, Jinan University, Guangzhou, China

Heterotrimeric G-proteins, comprising Gα and G$\beta\gamma$ subunits, couple metabotropic receptors to various downstream effectors and contribute to assembling and trafficking receptor-based signaling complexes. A G-protein β subunit, Gβ_3, plays a critical role in several physiological processes, as a polymorphism in its gene is associated with a risk factor for several disorders. Retinal ON bipolar cells express Gβ_3, and they provide an excellent system to study its role. In the ON bipolar cells, mGluR6 inverts the photoreceptor's signal via a cascade in which glutamate released from photoreceptors closes the TRPM1 channel. This cascade is essential for vision since deficiencies in its proteins lead to complete congenital stationary night blindness. Here we report that Gβ_3 participates in the G-protein heterotrimer that couples mGluR6 to TRPM1. Gβ_3 deletion in mouse greatly reduces the light response under both scotopic and photopic conditions, but it does not eliminate it. In addition, Gβ_3 deletion causes mislocalization and downregulation of most cascade elements and modulators. Furthermore, Gβ_3 may play a role in synaptic maintenance since in its absence, the number of invaginating rod bipolar dendrites is greatly reduced, a deficit that was not observed at 3 weeks, the end of the developmental period.

Introduction

Heterotrimeric G-proteins comprising Gα and G$\beta\gamma$ subunits are central to all cascades that are initiated by G-protein-coupled (metabotropic) receptors. Upon binding their ligand, these receptors activate their G-protein and modulate downstream effectors. The downstream effectors (enzymes or channels) modulate diverse processes ranging from growth and differentiation to normal physiological and signal processing. Historically, the α subunit of the G-protein has been considered to be the signal carrier, while the $\beta\gamma$ dimer has been thought to be its partner that suppresses the spontaneous signaling and provides a membrane anchor for the α subunit. However, accumulating data now show that in many signaling cascades, G$\beta\gamma$ interacts directly with different effectors. Furthermore, G$\beta\gamma$ contributes to the assembly and trafficking of receptor based signaling complexes, vastly expanding the range of signaling repertoire that is covered by G-proteins (for review, see Bomsel and Mostov, 1992; Dupré et al., 2009).

In retina, an important G-protein-mediated signaling cascade initiated by mGluR6 in the ON class of bipolar cells inverts the photoreceptor's hyperpolarizing light signal to a depolarizing response. Mutations in several of the cascade's proteins lead to complete congenital stationary night blindness. This condition can be diagnosed by the absence of the electroretinogram (ERG) b-wave, a compound potential that indicates ON bipolar cell activity. When glutamate activates mGluR6 on these cells in the dark, the heterotrimeric G-protein, G_o, becomes active. Active G_o then closes the nonselective cation channel TRPM1 via an unidentified mechanism (for review, see Koike et al., 2010a; Morgans et al., 2010). The dominant α subunit of G_o is $G\alpha_{o1}$, but $G\alpha_{o2}$ also contributes to the light response (Dhingra et al., 2000, 2002; Okawa et al., 2010). The strongest candidates for the G$\beta\gamma$ dimer in ON bipolar cells are Gβ_3 and Gγ_{13} since they localize to these cells (Lee et al., 1992; Peng et al., 1992; Huang et al., 2003). Gβ_3 is particularly interesting since polymorphism in this subunit has been associated with multigenic disorders—including hypertension, obesity, dyslipidemia, Alzheimer's disease, tumor progression, and others—and is being considered as a marker to predict disease risk and drug responsiveness (for review, see Weinstein et al., 2006). However, ON bipolar cells also express a divergent β subunit, Gβ_5, that in native tissue (brain and retina) forms a complex with the R7 family of regulator of G-protein signaling (RGS) molecules and not with Gγ (Witherow et al., 2000; Rao et al., 2007; Grabowska et al., 2008). Gβ_5 plays a key role in stabilizing its RGS partner in these bipolar cells, and deletion of the gene encoding Gβ_5 (*Gnb5*) eliminates the ERG b-wave. Given the diverse role of G-proteins and the critical role

Received March 22, 2012; revised June 21, 2012; accepted June 30, 2012.

Author contributions: A.D., A.L., and N.V. designed research; A.D., H.R., A.N., M.E.F., Y.X., J.L., D.C.C., and A.L. performed research; A.D., H.R., A.N., M.E.F., Y.X., and N.V. analyzed data; A.D. and N.V. wrote the paper.

This work was supported by National Institutes of Health Grants EY11105 (N.V.) and NEI P30 EY01583 (Vision Research Core of the University of Pennsylvania). We thank Cheshta Dhingra for helping to quantify the electron micrographs; Chidambaram Chinniah for helping with immunostaining and Western blotting; Dr. Gustavo Aguirre for helpful discussion; Dr. Rukmini Rao-Mirotznik for editing this manuscript; Drs. Takahisa Furukawa, Flockerzi Veit, Kirill A. Martemyanov, Robert Margolskee, Theodore G. Wensel, Vadim Y. Arshavsky, Shigetada Nakanishi, David Manning, and Catherine W. Morgans for donating the antibodies used in this study; Dr. Jason Chen for donating the *Gnb5*-null tissue and sharing images of *Gnb5*-null retinas stained for Gβ_3; and Dr. Robert Margolskee for donating fixed eyes from the *Gus8.4GFP* mouse.

Correspondence should be addressed to Anuradha Dhingra, Department of Neuroscience, 123 Anat-Chem Building, University of Pennsylvania, Philadelphia, PA 19104-6058. E-mail: dhingra@mail.med.upenn.edu.

DOI:10.1523/JNEUROSCI.1436-12.2012

 0270-6474/12/3211343-13$15.00/0

of ON bipolar cells in night vision, it is important to identify and test the function of the partners of $G\alpha_o$ in these cells.

In this study, we show that $G\beta_3$ is present in all ON bipolar cells, it forms the G-protein heterotrimer that couples mGluR6 to TRPM1, and its absence greatly diminishes the light response. Though a residual light response does remain, absence of $G\beta_3$ triggers a chain of events that mislocalizes and reduces expression of most cascade elements including the three subunits of the GTPase activating protein (GAP) complex. Furthermore, this malfunctioning alters the organization of the rod to rod bipolar synapse. These results demonstrate a remarkable new role for an important G-protein subunit in synaptic maintenance.

Materials and Methods

Generation and characterization of the Gnb3-null mouse. *Gnb3*+/− mice were produced by the Knockout Mouse Project (Davis, CA). Briefly, homologous recombination was performed using a large bacterial artificial chromosome-based targeting vector containing Velocigene cassette ZEN-Ub1 in place of the *Gnb3* coding region, and this resulted in deletion of the coding region in the ES cells. Germline transmission of the ES cell clones was confirmed by PCR. The absence of $G\beta_3$ protein in the null retina was confirmed by Western blotting (Fig. 1). Attempts to breed the *Gnb3*-null mice were not successful, so the heterozygous mice were bred to produce the null mice. The weight of the *Gnb3*-null adults varied, ranging from 7 to 15 g compared to 15 to 20 g for wild-type (WT) littermates. *Gnb3*-null mice had a higher mortality rate than wild-type or heterozygous littermates, as only ~10% of the pups had the null genotype at ~3 weeks. No other obvious phenotype was detected.

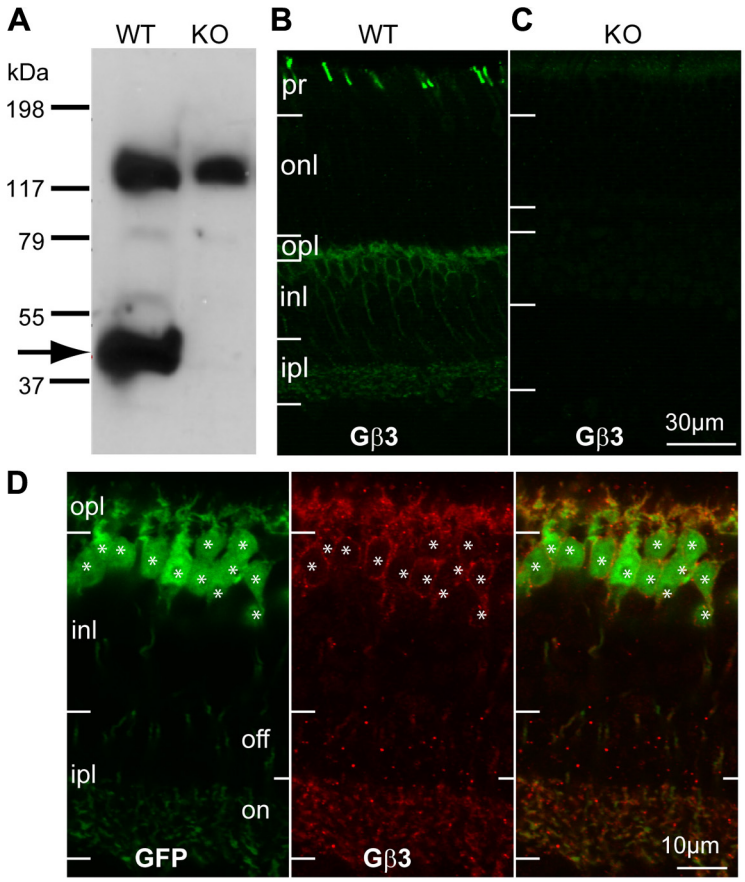

Figure 1. $G\beta_3$ is expressed by cones and all types of ON bipolar cells. ***A***, Western blots for $G\beta_3$ in WT and *Gnb3*-null (KO) mice show a specific band at the expected molecular weight of 38 kDa (arrow) and a higher nonspecific band at ~130 kDa. ***B***, Immunostaining for $G\beta_3$ in wild-type shows strong staining of cone outer segments (in the photoreceptor layer) and weaker staining in the outer plexiform layer and the inner nuclear layer. ***C***, All staining is absent in the null mouse. ***D***, Higher magnification of the stained inner retina of the *Grm6-GFP* mouse that expresses GFP in all and only ON bipolar cells. Strong $G\beta_3$ staining appears in the dendrites and somas, and weak staining is present in the ON sublamina of the inner plexiform layer (ipl). Note that all GFP-expressing cells also express $G\beta_3$ (asterisks) and vice versa. pr, Photoreceptor layer; onl, outer nuclear layer; opl, outer plexiform layer; inl, inner nuclear layer.

Other mouse genotypes or tissues. WT C57BL/6J mice were purchased from Charles River Laboratories; the *Grm6-GFP* mouse was generated in the lab as described previously (Morgan et al., 2006; Dhingra et al., 2008); the *Grm6*-null mouse was a gift from S. Nakanishi (Kyoto University, Kyoto, Japan) and D. Copenhagen (University of California, San Francisco, CA) and was described by Masu et al. (1995).

Dissection. Mice were treated in compliance with federal regulations and University of Pennsylvania policies. Mice were deeply anesthetized by intraperitoneal injection of a mixture of 85 μg/g ketamine and 13 μg/g xylazine; the eyes were enucleated, and the mice were killed by anesthetic overdose. Fixed retinas for *Gnb5*-null (and corresponding wild-type) mice [described previously by Rao et al. (2007)] were obtained from J. Chen (Virginia Commonwealth University, Richmond, VA). Fixed retinas of *Gus:8.4GFP* mice were obtained from R. Margolskee (Monell Institute, Philadelphia, PA). For all genotypes, both male and female mouse tissues were used.

Immunocytochemistry. Eyes were enucleated from an anesthetized mouse, and a small cut was made through each lens. Each eyeball was fixed in 4% paraformaldehyde for 10, 30, or 60 min, rinsed in phosphate buffer, soaked overnight in 30% buffered sucrose, and embedded in a mixture of two parts 20% sucrose in phosphate buffer and one part tissue freezing medium. The eyes were cryosectioned radially at 10–15 μm thickness. Sections were soaked in diluent containing 10% normal goat serum, 5% sucrose, and 0.5% Triton X-100 in phosphate buffer. These sections were then incubated in primary antibodies at 4°C overnight, washed, incubated for 3 h in secondary antibodies conjugated to a fluorescent marker, rinsed, and mounted in Vectashield (Vector Laboratories).

Imaging and quantification. Detailed quantification methods were described previously (Xu et al., 2012). Briefly, sections were photographed with an Olympus FV-1000 confocal microscope under a 40× or 60× oil-immersion objective. Immunostaining intensities were compared between age-matched wild-type and null retinas that were simultaneously processed and imaged under the same settings. Retinas that were processed in parallel were considered a set. Intensity measurements were taken from *z*-stacks (1 μm apart; same number of sections for wild-type and null mice) using Volocity software (Improvision). Regions of interest were drawn in the different layers, and the mean background intensity level (measured from the outer nuclear layer) was subtracted from the mean intensities of the regions of interest. The ratio of the mean intensities between paired wild-type and null mice was calculated for each region, and these ratios were averaged across three to five pairs (or sets). The number of puncta was assessed with the aid of Volocity software in a region of interest that encompassed the outer plexiform layer throughout the *z*-stack. The Volocity program counted every puncta that had a volume within a preset range and was more intense than a predefined threshold value. These values were adjusted for the wild-type retina to include every puncta judged by the experimenter to represent a dendritic tip, and the same values were then used for the null retina of that set. Paired Student's *t* test was used to compare the intensities between wild-type and null mice. We chose to use a paired *t* test to control for the variability within a genotype that may arise from minor differences in experimental conditions and imaging set-

tings done on different days. (An example of variability within a genotype for puncta count is given in Figure 6*C*).

Western blotting. Retinas were detached quickly from anesthetized mice and frozen in liquid nitrogen. Tissue was homogenized using a Polytron homogenizer in a lysis buffer containing 5 mM Tris-HCl, pH 7.5, 320 mM sucrose, 2 mM EDTA, 2.5 mM 2-mercaptoethanol, and protease inhibitor cocktail (P 8340; Sigma). Homogenate was centrifuged at 6000 × *g* for 10 min, and the supernatant was collected. Protein assays were performed using BSA protein reagent (Bio-Rad). The proteins were run on 7.5, 10, or 4–15% SDS-PAGE gels and transferred to a nitrocellulose membrane using a wet transfer apparatus (Bio-Rad). After a brief rinse in PBS, the blots were incubated sequentially in the following: Odyssey blocking buffer diluted with PBS (1:1, blocking buffer) at room temperature for 1 h; primary antibody diluted in blocking buffer containing 0.1% Tween 20 at 4°C overnight; washes in PBS plus 0.1% Tween 20 (PBST); IRDye-conjugated secondary antibodies (LI-COR Biosciences or Rockland, 1:15,000 dilution in blocking buffer containing 0.1% Tween 20) at room temperature for 1 h; washes in PBST; and a final rinse in PBS. The blots were then scanned using the Odyssey Infrared Imaging System (LI-COR Biosciences) according to manufacturer's instructions. To control for equal loading, we incubated blots simultaneously with antibodies against the test protein and against an internal control protein (e.g., β-actin). The band intensities were quantified using Odyssey software, adjusted for background and normalized against β-actin levels. For mGluR6, a chemiluminescence based detection method was used. Briefly, the blot was blocked in 5% milk in PBST followed by overnight incubation in primary antibody and 3 h incubation in anti-rabbit-HRP secondary antibody diluted in blocking buffer. The blot was developed for visualization using SuperSignal West Pico Chemiluminescent Substrate (Pierce).

Antibodies. Rabbit anti-Gβ_3 (1:300; HPA005645; Sigma), sheep anti-mGluR6 (1:100; a gift from C. Morgans, Oregon Health and Science University, Portland, OR), mouse anti-Gα_o (1:100; MAB 3073; Millipore), rabbit anti-Gγ_{13} (1:500; a gift from R. Margolskee), rabbit anti-TRPM1 (1:100; a gift from T. Furukawa, Osaka Bioscience Institute, Osaka, Japan), rabbit anti-Gβ_5 (1:500) and rabbit anti-RGS11 (1:1000; gifts from T. Wensel, Baylor College of Medicine, Houston, TX), rabbit anti-RGS9 anchor protein (R9AP) (1:1000; a gift from V. Arshavsky, Duke University, Durham, NC), rabbit anti-PKC (1:1000; Sigma; catalog #P4334), and rabbit anti-retinal Purkinje cell protein 2 (Ret-PCP2; 1:1000; a gift from R. Feddersen, Mayo Clinic, Rochester, MN) (Xu et al. 2008) were used. For certain proteins, Western blotting worked only (or better) with a different antibody. Thus, for this application, we used rabbit anti-Gβ_3 (1:250; Santa Cruz Biotechnology; catalog #sc381), sheep anti-TRPM1 (1:1000; a gift from K. Martemayanov, Scripps Research Institute, Jupiter, Florida), rabbit anti-Gα_o (1:3000; a gift from D. Manning, University of Pennsylvania, Philadelphia, PA), and mouse anti-β-actin (1:3000; Clone AC-74; Sigma).

Electroretinographic recordings. The electroretinographic recording methods have been described in detail previously (Lyubarsky et al., 1999, 2000; Ng et al., 2010). Briefly, an adult mouse was dark adapted overnight and then anesthetized under dim red light by intraperitoneal injection of a mixture containing (in mg/g body weight) 20 ketamine, 8 xylazine, and 800 urethane, and placed onto a platform maintained at 38°C. The pupils were dilated with 1% tropicamide saline solution (Mydriacyl; Alconox). A platinum recording electrode was placed in contact with the cornea, and another platinum wire electrode placed into the mouth was used as both the reference and ground electrode. The mouse was then placed inside a light-proof Faraday cage that also served as a ganzfeld, with appropriate ports and baffles to ensure uniform illumination. The light stimuli were either 4 ms flashes produced by a light-emitting diode (LED) stimulator or <1 ms flashes produced by a Xenon tube delivered in the ganzfeld (Espion Electrophysiology System; Diagnosys). Light intensities were converted to the estimated number of photoisomerizations (R^*) per photoreceptor as described previously (Lyubarsky et al., 1999, 2000, 2004). ERGs were recorded from both eyes using differential amplifiers with a bandwidth of 0.1 Hz to 1 kHz, and were sampled at 1 ms intervals. A typical record was an average of 3 to 25 individual responses (depending on the signal-to-noise ratio).

To quantify the ERG b-wave, we determined in the wild-type mice for each condition (scotopic, mixed, and photopic) the time range at which the ERG b-wave reached its peak. These time windows were 75–140 ms after the flash for scotopic stimuli, 60–105 ms for the mixed rod and cone ERG with the saturating stimulus, and 40–90 ms for photopic stimuli. We then averaged the ERG values of each record over this time window to obtain a representative value for the "peak" potential. These values were compared between *Grm6*- and *Gnb3*-null mice. To extract the b-wave, we averaged these numbers across all tested *Grm6*-null animals in each condition to obtain the magnitude of the a-wave in the absence of a b-wave. Subtracting this *Grm6*-null average value from the average of wild-type or *Gnb3*-null retinas provides a reliable estimate of the b-wave. Averages over all records from WT minus *Grm6*-null and *Gnb3*-null minus *Grm6*-null were then compared with a two tailed Student's *t* test. To test the effect of L-AP4 on the b-wave, we performed ERG recordings on the WT and null mice before and after injection of the drug. The injections were performed under infrared illumination; 3 μl of 10 mM L-AP4 was injected intravitreally into one eye, and same volume of saline (control) was injected into the other eye. The postinjection ERG was done 30–70 min later.

Whole-cell recording, light stimulus, and data analysis. Retinal slices were prepared as described previously (Xu et al., 2008). Briefly, retinas were isolated and cut into 200-μm-thick slices with a tissue slicer (Narishige). Slices were transferred to a recording chamber, secured with vacuum grease, and then moved to the microscope stage of an Olympus microscope. The chamber was perfused at a rate of 0.5–1 ml/min with oxygenated (95% O_2, 5% CO_2) Ames medium (Sigma) containing sodium bicarbonate (1.9 g/L) at 32–34°C. Patch pipettes with resistances of 5–7 MΩ were fabricated from borosilicate glass using an electrode puller (Sutter Instrument). Pipettes were filled with a solution containing the following (in mM): 110 K-gluconate, 10 EGTA, 10 HEPES, 10 KCl, 5 NaCl, 4 MgATP, and 1 LiGTP; pH was adjusted to 7.4 with KOH, and osmolality was 290 mOsmol. All chemicals were obtained from Sigma. Whole-cell recordings were obtained with an Axopatch 1D amplifier (Molecular Devices). Membrane potentials were corrected for the liquid junction potential that was calculated to be ~15mV. Cells were discarded if the baseline current exceeded −100 pA at a holding potential of −60 mV. Voltage command generation and data acquisition were accomplished with Clampex (Molecular Devices). Cells were either current clamped with zero current injection to measure the resting membrane potential or voltage clamped to measure the I–V curve and current noise. The retina was stimulated using full-field light generated by an LED with a peak wavelength of 565 nm. The light illuminance ranged from 1.37E+03 to 2.53E+05 photons/μm^2/s. For each cell, a sequence of increasing light intensities was repeated three times, and the recordings were averaged using Igor software (WaveMetrics). The averaged responses are displayed in Results as recording traces. Waveform analysis of these responses was done off-line with Clampfit (Molecular Devices). Resting membrane potential was determined by averaging the voltage values during the first 1 s period of recorded spontaneous activity. Current noise was defined as the SD of the spontaneous activity during this first second of recording while the cell was voltage clamped at −60 mV. Results for wild-type and null mice were compared with a Student's *t* test. Differences were considered significant at $p \leq 0.05$. All data are reported as the mean ± SEM.

Quantitative real-time PCR. Total RNA from mouse retina was isolated with a Nucleospin RNA II kit (Macherey-Nagel). cDNA was synthesized with a high-capacity cDNA reverse transcription kit (Applied Biosystems). Quantitative real-time PCR was performed with a Power SYBR Green kit (Applied Biosystems) on an Applied Biosystems 7500 Fast Real-Time PCR System. Melt curve analysis verified the specificity of the product. GAPDH was used as a reference gene for normalization, and analysis of relative gene expression was performed using the relative standard curve method per the manufacturer's protocol.

The primers were as follows: *Grm6* NM_173372.2, forward position, (143) 5′ GAGGTTGGCTCAGTCCAGGAGCA; reverse, (240) CCCGCACC GTGAGCTATGCC; *Nyx* NM_173415.4, forward, (196) AGGTGCAAGG AAGGCCAAGGGA; reverse, (247) AGACCACCGCATGAAGAAGCAGG; *Trpm1* NM_001039104.2, forward, (219) AGCAGCTCCTTCAAGCGTG GTTCA; reverse, (285) ATGCTTTCTGACCCTTCTGGGACCC; Gng13 NM_022422.5, forward, (32) GGACTCGGACAGCCCAGCCT; reverse, (118) GCCAGCCTGAGGTTTTGGAGGAGA; GAPDH NM_008084.2, forward, (5) ACGGCCGCATCTTCTTGTGCA; reverse, (85) ATACGG-CCAAATCCGTTCACACCG.

Immunoprecipitation. Mouse retinas were homogenized in RIPA buffer (R0278; Sigma) with 1 mM 2-mercaptoethanol, 1 mM EDTA, 1 mM GDPβS, and protease inhibitors (P 8340; Sigma) at low speed and centrifuged at 8000 × *g* for 5 min. The supernatant was precleared by adding 20 μl of protein G-agarose beads (Invitrogen) and was incubated with mouse anti-$G\alpha_o$ and protein G-agarose beads on a rotator at 4°C overnight. The beads with protein complexes were pulled down by centrifugation (10,000 × *g*), washed thoroughly in homogenization buffer, resuspended in Laemmli buffer, and boiled. The supernatant was then run on a 4–15% SDS PAGE gel. The protein was transferred to a nitrocellulose membrane, and the blot was probed for rabbit anti-$G\alpha_o$, anti-$G\beta_3$, or anti-$G\beta_5$.

Electron microscopy. Eyes were fixed in 0.1 M phosphate buffer, pH 7.4, containing 2% paraformaldehyde and 2% glutaraldehyde for 6–12 h. Eyes were then rinsed in phosphate buffer, and small pieces of retina were taken (with the optic disk at one end). Tissues were incubated in 2% osmium tetroxide in 0.1 M phosphate buffer for 2 h, rinsed with phosphate buffer, dehydrated in series of ethanol, and incubated sequentially with Embed 812/propylene oxide mixtures (1:1 and 2:1) and pure Embed 812 mixture (Electron Microscopy Sciences) overnight. Tissues were then embedded in fresh Embed 812 mixture at 60°C for 48 h. Semithin sections (1 μm) were stained with toluidine blue. Ultrathin sections (90 nm) were counterstained with uranyl acetate and lead citrate and examined with a JEM 1011 transmission electron microscope. Images were captured with an ORIUS 835.10W CCD camera (Gatan).

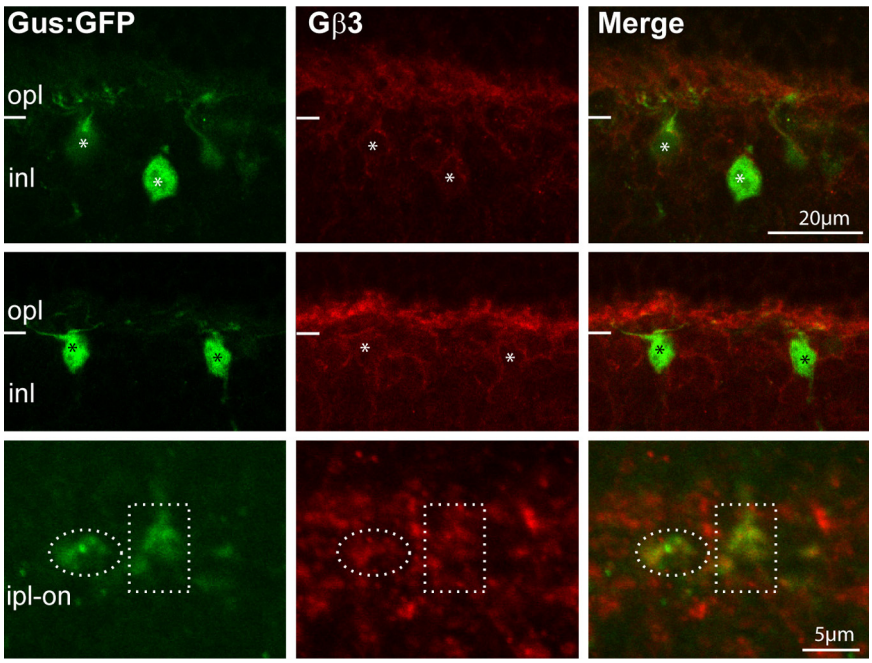

Figure 2. Type 7 cone bipolar cells express $G\beta_3$. A retina of a transgenic mouse, *Gus8.4GFP* (which expresses GFP weakly in certain rod bipolar cells and strongly in type 7 cone bipolar cells), stained for $G\beta_3$ shows that bright GFP-labeled somas are stained for $G\beta_3$ (asterisks). Dotted ellipses encircle type 7 axon terminals in the ipl, and these terminals are weakly stained for $G\beta_3$. Abbreviations are defined as in Figure 1.

Results

$G\beta_3$ is expressed in cones and all types of ON bipolar cells

The general localization of $G\beta_3$ in mouse retina has been described previously (Lee et al., 1992; Peng et al., 1992; Huang et al., 2003; Ritchey et al., 2010). Here, using Western blots and immunostaining of the *Gnb3* (gene encoding $G\beta_3$)-null mouse, we tested the authenticity of these reports and further determined the detailed expression pattern. Western blots of wild-type retina showed two strong bands: a band at the expected size of 38 kDa, which is diminished in the *Gnb3*-null mouse, and a nonspecific one at ~130 kDa (Fig. 1*A*). Wild-type immunostaining was strong in cone outer segments and somewhat weaker in bipolar cells; all of this staining was eliminated in the null mouse (Fig. 1*B*,*C*). In the *Grm6-GFP* mouse, where all types of ON bipolar cells were labeled, $G\beta_3$ was expressed by all and only bipolar cells of the ON type (Fig. 1*D*). To further support this assessment, we stained for $G\beta_3$ in the *GUS8.4GFP* retina, where GFP expression is strong in type 7 cone bipolar cells and weak in some rod bipolar cells (Huang et al., 2003). We found that all somas and dendrites that expressed GFP appeared stained for $G\beta_3$. To differentiate type 7 cone bipolar cells from rod bipolar cells, we examined the axon terminals in stratum 3 of the inner plexiform layer, where type 7 cells arborize and can be differentiated from the rod bipolar axon terminals that arborize in stratum 5. These type 7 terminals showed faint but clear expression of $G\beta_3$ (Fig. 2).

To examine the general morphology of the *Gnb3*-null retina, we studied 1-μm-thick plastic sections stained with toluidine blue. All retinal layers of this mouse appeared normal in thickness, and most cells exhibited normal size and appearance (Fig. 3). In certain areas, we noticed wider spaces between cells, possibly due to Muller cell proliferation. To assess cell morphology, we labeled different cell types with standard markers: photoreceptors with recoverin, horizontal cells and certain amacrine cells with calbindin, synaptic layers with synaptophysin, and cholinergic amacrine cells with choline acetyl transferase. All gross cell morphologies revealed by these markers appeared normal (Fig. 4).

Gnb3-null ON bipolar cells have a residual light response

We tested the light response of ON bipolar cells by recording ERGs in response to light flashes. Under dark adaptation with scotopic stimuli, the a-wave is generally undetectable so the ERG mainly displays a positive-going b-wave that is generated by rod bipolar cells. In the *Gnb3*-null mouse, the ERG showed no clear positive-going wave (Fig. 5*A*). With a saturated light stimulus, the dark adapted mouse eye generates a mixed rod- and cone-generated signal. In wild types, this ERG trace comprised a saturated negative-going a-wave (indicating photoreceptor activity) and a positive-going b-wave (indicating mixed activity in rod and ON-cone bipolar cells). In the *Gnb3*-null mouse, the clear positive wave was absent (Fig. 5*B*). The initial phase of the negative wave (the a-wave) appeared normal (Fig. 5*B*), but its shape differed from that of a *Grm6*-null retina, which completely lacks ON bipolar cell activity (Masu et al., 1995). In the *Grm6*-null mouse, after a fast transient response, the a-wave stayed at a plateau level for ~200 ms before returning to the baseline. In the *Gnb3*-null mouse, the negative wave started to rise soon after reaching its peak. To see if the difference between the two genotypes is genuine, we averaged point values in a time window where the wild-type b-wave peaks (see Materials and Methods) (Fig. 5, right); the difference was significant ($p < 0.05$ for scotopic flash intensities, and $p < 0.01$ for saturated flash intensities). This suggests that at least some ON bipolar cells have a residual response that pulls the a-wave toward positive values. To extract this residual b-wave, we

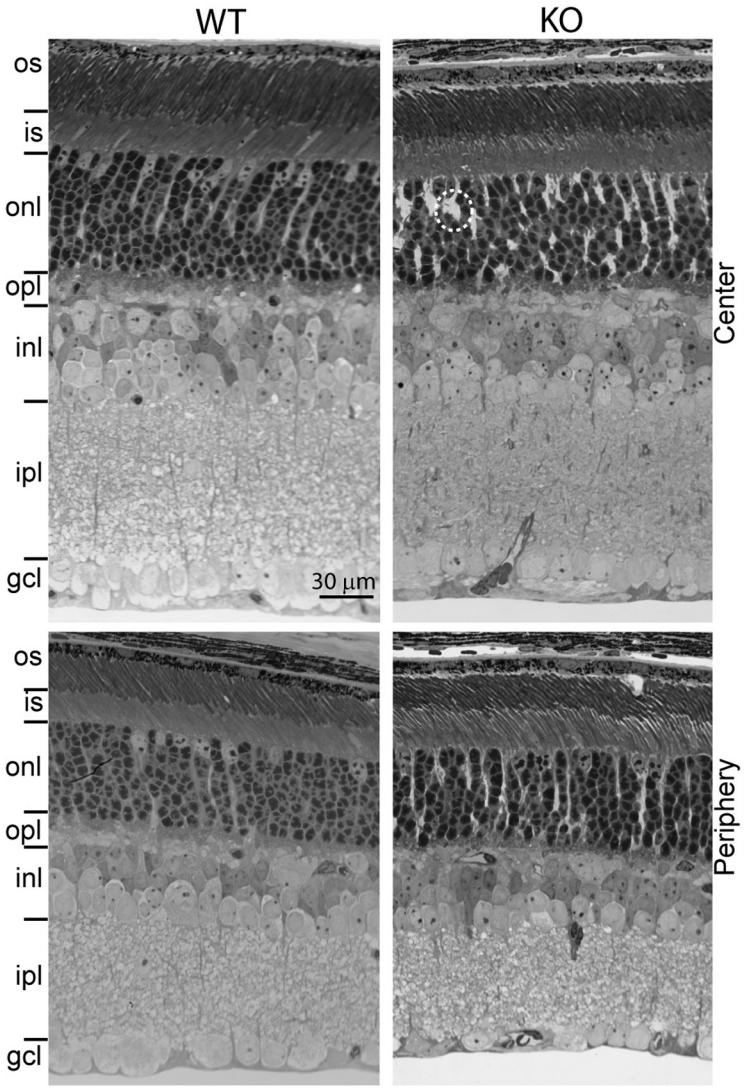

Figure 3. Retinal layers of wild-type and *Gnb3*-null mice have similar appearance and thickness. Semithin (1 μm; radial view) epon radial sections of retinas (4 weeks old) stained with toluidine blue clearly show all the retinal layers. This picture is representative of three adult WTs and three adult KOs. The layers in general have a normal appearance, but in certain regions, Muller cells appear to occupy bigger spaces than normal (within the dotted circle). Top panels show the center of the retina, and bottom panels show the periphery. os, Outer segments; is, inner segments; gcl, ganglion cell layer. Other abbreviations are defined as in Figure 1.

assumed that the average a-wave of the *Gnb3*-null mouse remained identical to that of the wild-type and *Grm6*-null mice. Our assumption was justified since the average peak a-waves in the three genotypes was similar (Fig. 5). Since the ERG of the *Grm6*-null mouse contains no b-wave, subtracting the *Grm6*-null ERG trace from that of the wild-type or *Gnb3*-null mouse should provide a pure b-wave for each of those genotypes (Robson and Frishman, 1995; Green and Kapousta-Bruneau, 1999). This idea was confirmed with the wild-type mice, where the subtracted records from scotopic and saturated luminances gave relatively pure positive-going b-waves (Fig. 5*A*,*B*, right). Performing this operation on ERGs obtained from *Gnb3*-null mice revealed the positive b-wave in this genotype (Fig. 5*A*,*B*, right). We have quantified the amplitudes of the b-wave by averaging the values over the same time windows mentioned above. This is necessary because the positive wave of the null mouse had no peak, i.e., it continued to go up much after the wild-type b-wave peaked. For both scotopic and saturated (mixed) conditions, the b-wave of the *Gnb3*-null mouse was reduced to 28% of that of the wild types (Fig. 5*F*).

If indeed *Gnb3*-null mouse shows a residual b-wave, we should be able to block it with L-AP4. We therefore performed ERG before and after injecting L-AP4 to one eye and a control saline to the other. Injection of either L-AP4 or saline reduced the a-wave to approximately half in both wild-type and *Gnb3*-null mice. As for the b-wave, injection of saline to the wild type reduced it, while L-AP4 eliminated it (data not shown). In the case of *Gnb3*-null eyes, injection of either of these agents eliminated the residual b-wave. This experiment was repeated on three animals of each genotype, and all showed the same results. Because the residual b-wave is small, and because the experimental procedure also had an effect on the b-wave, it is hard to decipher the reduction specific to L-AP4.

To further probe the responses of rod bipolar cells, we performed whole-cell recordings on rod bipolar cells in current- and voltage-clamp modes. We recorded from 24 cells in a *Gnb3*-null retina and found that two gave a small response to a strong light flash (Fig. 5*E*). This response was dramatically lower than that observed in wild-type retina, where 14 of 25 cells showed nice responses (Fig. 5*D*). Unlike *Grm6*-null cells, whose resting potential is more hyperpolarized than that of wild type and whose channel activity is lower (Xu et al., 2012), *Gnb3*-null rod bipolar cells had a slightly (but insignificantly) more depolarized resting potential and similar noise level as the wild-type cells (Table 1). Thus, even though the light response is almost eliminated, the TRPM1 channel retains detectable activity, and the cascade that is triggered by glutamate to close the TRPM1 channel retains some residual functionality.

To measure cone-driven (photopic) responses in *Gnb3*-null mice, we suppressed rod responses by light adaptation, presented a strong light stimulus, and recorded ERGs. Surprisingly, even though cones are known to express Gβ_3, the saturated cone-driven negative-going wave of these knockout (KO) mice appeared normal with amplitudes that were similar to those of wild-type and *Grm6*-null mice (Fig. 5*C*). Similar to the mixed rod and cone ERG wave, the saturated cone-generated negative ERG phase rose faster than the *Grm6*-null photopic a-wave, suggesting a contribution from a residual b-wave. Since the peak of the saturated cone-driven negative wave was similar to that of wild-type mice, we again subtracted the photopic *Grm6*-null ERG to obtain the cone-driven b-wave of the *Gnb3*-null mouse. This residual b-wave was reduced to 22% of the wild-type b-wave (Fig. 5*F*). The greater reduction in cone-generated b-wave compared to rod-generated b-wave may be due to reduced responses in cones (our unpublished data).

To test whether the residual light response in *Gnb3*-null mice is due to upregulation of a different Gβ subunit in the absence of

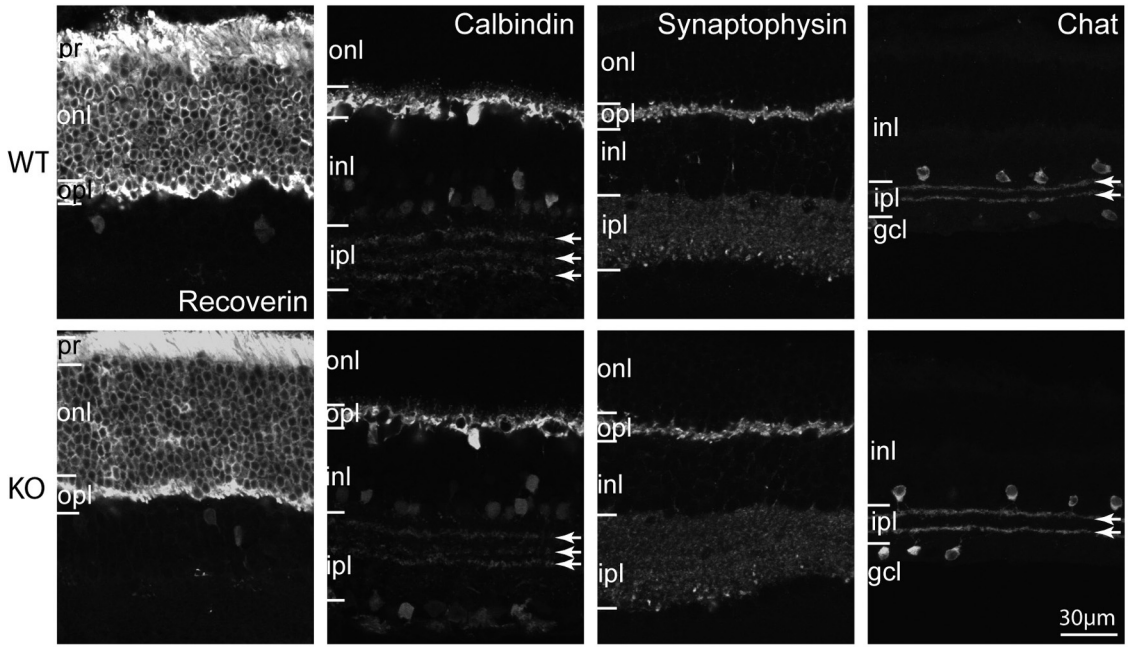

Figure 4. Gross morphology of all cell classes is normal in the *Gnb3*-null retina. Immunostaining using several cell markers for WT (top) and *Gnb3*-null (KO; bottom) retinas. Recoverin labels all photoreceptors throughout the cell including outer and inner segments, somas, and photoreceptor terminals. All of these segments are stained in both wild-type and null retinas. Calbindin labels horizontal cells strongly and certain amacrine cells weakly. Horizontal cells and the three bands in the ipl (arrows) appear similar. Synaptophysin staining shows that the two synaptic layers are similar. Choline acetyl transferase (Chat) labels the cholinergic amacrine cells that stratify in the OFF (top band) and ON sublaminas (lower band) of the ipl; these bands are unaffected by the absence of $G\beta_3$. Data are representative of three (synaptophysin) to eight (calbindin) images from three different animals for each genotype. Abbreviations are defined as in Figure 1.

$G\beta_3$, we immunostained for the other known $G\beta$s. Staining for $G\beta_1$ gave a strong staining in rods but not in ON bipolar cells. Staining for $G\beta_2$ and $G\beta_4$ was also negative in ON bipolar cells or any cell in the retina (data not shown). Staining for $G\beta_5$ was actually decreased and will be described below.

$G\beta_3$ is required for the normal expression of the key components of the mGluR6 cascade

When the elimination of a protein affects the expression of another protein expressed in its vicinity, the common interpretation is that these proteins interact. Such is the case for nyctalopin, whose absence reduces TRPM1 expression; mGluR6, whose absence reduces TRPM1, $G\beta_5$ and RGS11 expression; and $G\beta_5$, whose absence affects R9AP, RGS7, and RGS11 expression (Cao et al., 2009; Pearring et al., 2011; Xu et al., 2012). We therefore tested which cascade elements are affected by the absence of $G\beta_3$.

We started with the G-protein subunits. It is known that $G\alpha_{o1}$ is required for the light response (Dhingra et al., 2002), so if it forms a heterotrimer with $G\beta_3$, it is expected to down regulate. In accordance, staining for $G\alpha_{o1}$, which is strong in the dendrites of wild-type ON bipolar cells and weaker in their somas, was greatly reduced in both the dendrites and somas of *Gnb3*-null ON bipolar cells (Fig. 6*A*). Quantifying the staining intensity in the outer plexiform and inner nuclear layers showed that intensity in each layer decreased to ~40% of that in wild type (Fig. 6*D*). Western blots showed that the band intensity decreased to 77% of that in wild type (Fig. 6*B*,*D*), a value that is consistent with the total reduction observed by immunocytochemistry. The apparent lower reduction in Western blot intensity or in overall immunocytochemistry intensity (sum) can be explained by the expression of $G\alpha_o$ in amacrine cells in addition to ON bipolar cells (Vardi et al., 1993). The $G\gamma$ candidate in ON bipolar cells is $G\gamma_{13}$ (Huang et al., 2003), and in wild type, this subunit is expressed only by ON bipolar cells throughout the cell. In *Gnb3*-null retina, $G\gamma_{13}$ staining in the outer plexiform and inner nuclear layers was reduced to ~40%, and that in the ON sublamina decreased to ~60% (Fig. 6*A*,*D*). Due to the low molecular weight of this protein, we could not perform reliable Western blotting. However, since $G\gamma_{13}$ is only expressed by ON bipolar cells in retina, the 50% overall (sum) reduction in intensity level by immunocytochemistry reflects the decrease in the ON bipolar cells.

We next examined expression of the receptor-channel complex. In wild type, the glutamate receptor mGluR6 is restricted to the ON bipolar dendritic tips. In the *Gnb3*-null retina, there was a sizeable reduction in this punctate staining. Overall staining intensity in the outer plexiform layer was reduced to ~60% of that in wild type. Since the staining in the null mouse did remain punctate, we also compared the number of puncta in the two genotypes; this number decreased to ~50% of that in wild type (Fig. 6*A*,*D*). Western blotting using the Odyssey system did not work for this protein, so we checked the expression level by chemiluminescence (Fig. 6*B*). The protein levels were lower in three experiments (not quantified). Expression of the obligatory channel TRPM1 also showed reduced expression. In wild type, this channel is expressed strongly in the dendritic tips in a punctate fashion, but it is also expressed in the somas and very weakly in the axon terminals. In the null retina, average intensity of TRPM1 staining in the outer plexiform layer decreased to 60% of that in wild type, and the number of puncta decreased to ~55% (Fig. 6*A*–*D*). Western blots showed that the band intensity in the null mouse decreased to 37% of that in wild type (Fig. 6*B*,*D*).

Next we tested the expression of known cascade modulators. Three modulators—$G\beta_5$, R9AP, and RGS11—are thought to be in a tight complex (Cao et al., 2009), and they are highly concentrated in the dendritic tips of the ON bipolar cells. In the null retina, the characteristic punctate staining of these three modu-

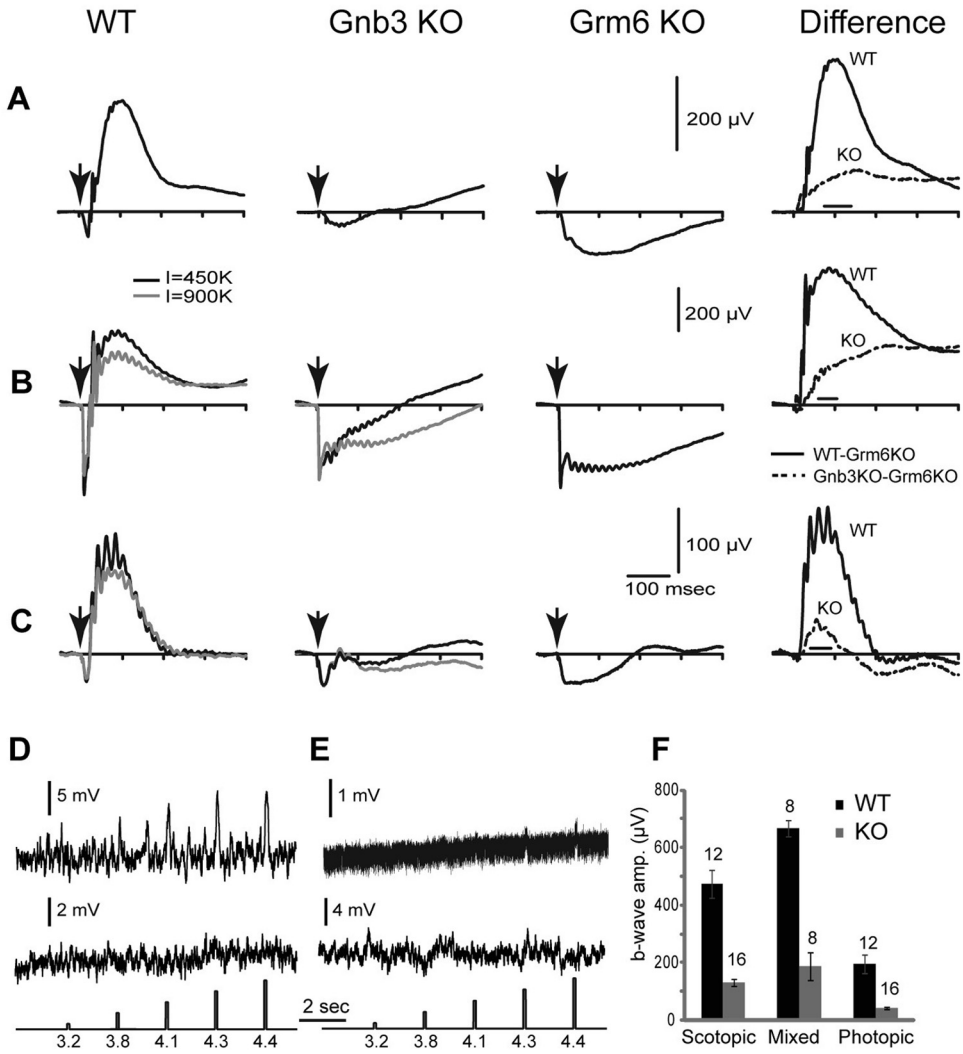

Figure 5. Light responses in *Gnb3*-null ON bipolar cells are dramatically reduced, but not eliminated. ***A–C***, Averaged ERGs of WT, *Gnb3*-null (KO), and *Grm6*-null (KO) mice under three different conditions. Arrows indicate a stimulus flash. In ***A***, animals were dark adapted overnight and stimulated with a flash that produced 10 photoisomerizations per rod, which is below cone threshold. These represent scotopic conditions. The right panel represents the average *Grm6* KO record subtracted from the average WT (solid lines) or *Gnb3*-KO record (dotted lines). This difference between the original ERG record and the *Grm6* KO record is an estimate of the pure b-wave in these two mouse lines. In ***B***, animals were dark adapted and stimulated with a saturated light flash of 450,000 (black traces) or 900,000 (gray) *R** per rod. This flash stimulates both rods and cones, so the ERG represents the mixed rod- and cone-driven responses. Subtracted records on the right are for the lower intensity (black). In ***C***, mice were adapted to a bright background (513 nm; 27,000 *R**/rod/s) that completely suppressed the cGMP-activated current of the rods. They were then stimulated with an intense white flash that isomerizes 1% of the M-cone pigment and 0.1% of the UV-cone pigment in adult mice. ERG traces represent cone-driven responses, i.e., photopic conditions. For the mixed and photopic responses (***B***, ***C***), only the records for 450,000 *R** per rod were used for subtraction (because the *Grm6*-KO was stimulated only with this intensity). The number of records averaged for *Grm6*-null mice was eight for scotopic and mixed conditions and six for photopic conditions. ***D***, ***E***, Whole-cell recordings from wild-type (***D***) and *Gnb3*-KO (***E***) rod bipolar cells under current-clamp mode. Two examples are given for each genotype; the top one shows a light response and the bottom does not. The response of the *Gnb3*-KO cell in the top trace is very small, but clearly above the noise. Interestingly, the noise level in this cell was much lower than the rest (same recording procedures). Perhaps this is the reason the response can be extracted. The lowest traces show the timing and intensity of the light stimuli; these are given in log photons μm^{-2} per flash. ***F***, A histogram quantifying the average b-wave amplitude for wild-type and *Gnb3*-null eyes under the three recording conditions. The time windows used to average these values for each condition are indicated by the horizontal line just above the *x*-axis in the difference ERGs of ***A–C***. Numbers above the histogram bars indicate the numbers of averaged records. For this and subsequent figures, error bars indicate SEs.

Table 1. Physiological characteristics of the resting rod bipolar cell

	Wild type (*n*)	*Gnb3* null (*n*)	*t* test value
Resting potential (mV)	−47.11 ± 4.74 (17)	−39.44 ± 3.57 (15)	0.22
Holding current (pA)	−9.15 ± 5.72 (25)	−24.96 ± 9.57 (24)	0.16
Voltage noise (mV)	1.85 ± 0.32 (17)	1.55 ± 0.19 (15)	0.44
Current noise (pA)	3.04 ± 0.61 (25)	2.75 ± 0.18 (24)	0.65

Channel activity obtained by whole-cell recording was similar in wild-type and *Gnb3*-null rod bipolar cells. Numbers are averages ± SE. Resting potential and voltage noise were measured when the current was clamped at 0 pA; holding current and current noise were measured when cells were clamped at −60 mV.

lators was diminished, and diffuse staining could occasionally be observed where primary dendrites coursed through the outer plexiform layer (Fig. 7*A*). The number of puncta in the outer plexiform layer was dramatically reduced to ~10% of that in wild type for both Gβ_5 and RGS11 and to 30% for R9AP (Fig. 7*B*). Since Gβ_5 and R9AP are heavily expressed in photoreceptors while RGS11 is restricted to ON bipolar cells (Chen et al., 2000, 2010; Krispel et al., 2003; Morgans et al., 2007; Jeffrey et al., 2010; Masuho et al., 2010; Zhang et al., 2010), we performed Western blotting only for RGS11 (Fig. 7*D*). We found that its expression was reduced to 73% of that in wild type (Fig. 7*B*).

Finally, we tested the expression pattern of two other modulators, protein kinase C α and Ret-PCP2 (Fig. 7*C*,*E*). PKC is expressed only by rod bipolar cells, where it is expressed relatively uniformly throughout the cell. Staining for PKC in the *Gnb3*-null mouse revealed reduced intensity compared to the wild type in both dendrites (60% of that in wild type) and axons (70%) of rod

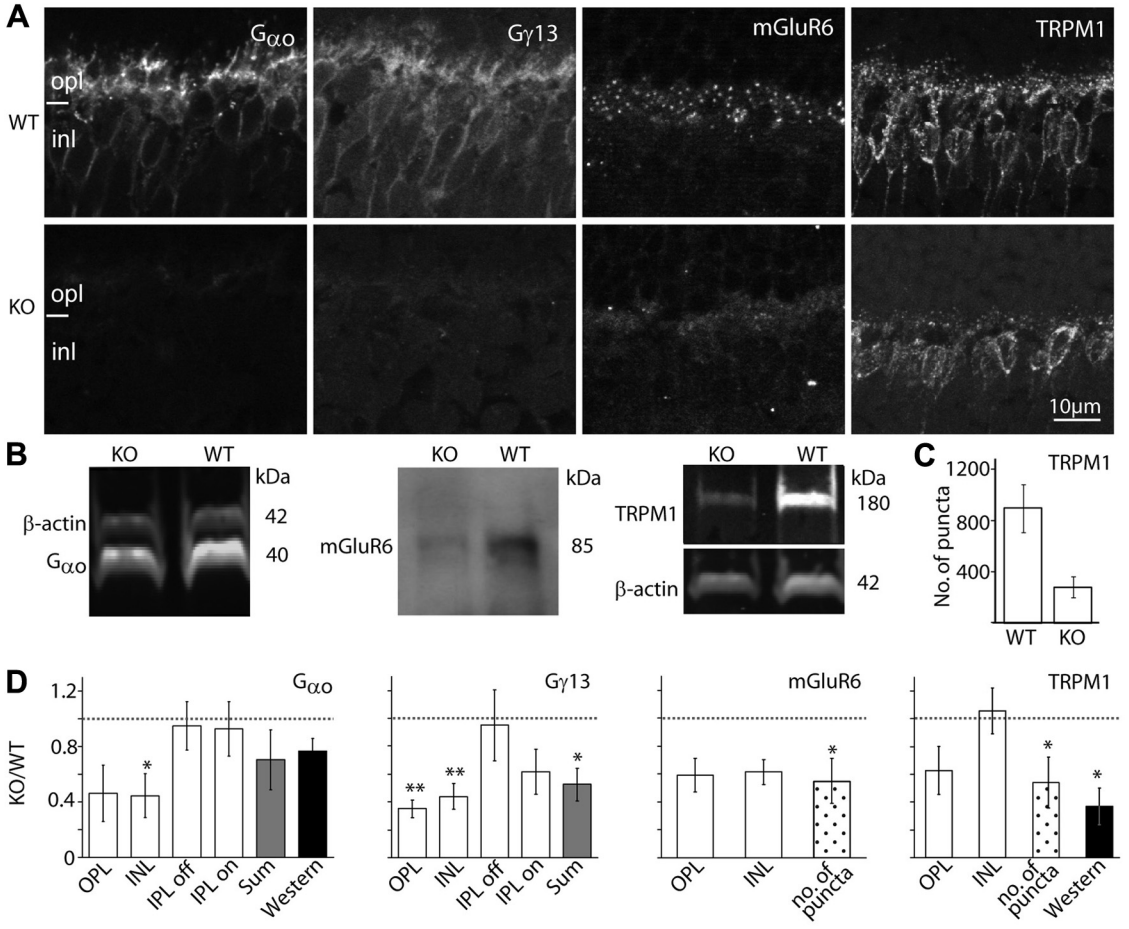

Figure 6. The essential cascade elements are down regulated. ***A***, Immunostaining of WT (top) and *Gnb3*-null (KO; bottom) retinas for $G\alpha_o$, $G\gamma_{13}$, mGluR6, and TRPM1. Staining in the null mouse was greatly reduced. ***B***, Western blots for $G\alpha_o$ and TRPM1 were done with the Odyssey reagents (bands are brighter than background), and for mGluR6 were performed with the ECL technique (bands are darker than background). Bands' identities and molecular weights are indicated on the sides of the blots. All three proteins are downregulated in the null mouse. ***C***, Bar chart showing the average number of TRPM1-positive puncta in the outer plexiform layer (within a retinal area of 1680 μm^2) in the WT and null retinas ($n = 3$ for each). ***D***, Relative immunostaining intensity (i.e., staining intensity in null divided by staining intensity in wild type) for various proteins in the layers of the retina (white bars), sum intensity of all layers (gray bars), and relative intensity of the protein bands (Western blots, dark bars). For staining patterns that show puncta in the opl, the relative number of puncta is also shown (dotted bars). $^*p < 0.05$; $^{**}p < 0.01$. Western blot quantification for mGluR6 was not performed because of the need to use ECL; however, in every set, the mGluR6 band in the null retina is less intense than that in wild type. The dotted horizontal line shows unity, i.e., when wild-type and null retinas are the same. All experiments were performed on at least three sets, where a set included a null and wild-type retina from littermates; when a littermate was not available, an age-matched wild type was used. For this and subsequent figures, the same settings are used for each pair of pictures. Abbreviations are defined as in Figure 1.

bipolar cells. The general morphology of the cells had fairly normal appearance with somas of similar size, and approximately the same density. The dendrites appeared shorter, probably because of failure to stain at the tip; the axons and axon terminals appeared normal. Ret-PCP2 is expressed in rod bipolar cells and several types of ON cone bipolar cells, and it is also expressed throughout the cell (Berrebi and Mugnaini, 1992; Xu et al., 2008). Staining for Ret-PCP2 in the outer plexiform layer of the *Gnb3*-null mouse was ~50% of that in wild-type, but staining of the inner retina did not change significantly.

In conclusion, deleting $G\beta_3$ affected most severely the modulators that cluster in the dendritic tips, followed by the G-protein subunits, then mGluR6 and TRPM1, and finally the diffusely distributed modulators. No compensatory expression of another $G\beta$ subunit could be detected.

mRNA for several cascade proteins in the *Gnb3*-null mouse is similar to that in wild-type

The downregulation of affected proteins can result from reduced mRNA synthesis or from posttranscriptional effect, e.g., degradation due to instability as has been suggested for the R9AP/RGS9/$G\beta_5$ complex in photoreceptors (for review, see Martemyanov and Arshavsky, 2009) and the R9AP/RGS7 (or RGS11)/$G\beta_5$ complex in bipolar cells (Cao et al., 2009). To determine whether the downregulation was at the transcriptional level, we performed quantitative real-time PCR. We primarily limited our analysis to messages that are restricted to ON bipolar cells, i.e., mGluR6, nyctalopin, $G\gamma_{13}$, and TRPM1. The ratios of the amplified message from the null retina to that of the wild-type were as follows: 0.64 ± 0.2 for mGluR6, 1.13 ± 0.3 for nyctalopin, 1.01 ± 0.36 for $G\gamma_{13}$, and 0.92 ± 0.1 for TRPM1 (four retinas of each genotype, triplicates per retina). Although the mRNA levels for mGluR6 seemed lower in the *Gnb3*-null retina, there was no statistically significant difference between the wild-type and *Gnb3*-null retinas for any of the messages tested.

$G\beta_3$ is required to maintain a typical rod synaptic tetrad

Given that so many cascade elements were downregulated in the ON bipolar cells, it was important to test whether their synaptic contacts with photoreceptors remained intact. We therefore evaluated the ultrastructure of the rod tetrad by carefully examining the EM micrographs of wild-type and *Gnb3*-null retinal sections that extended from the center to the periphery. We found that the

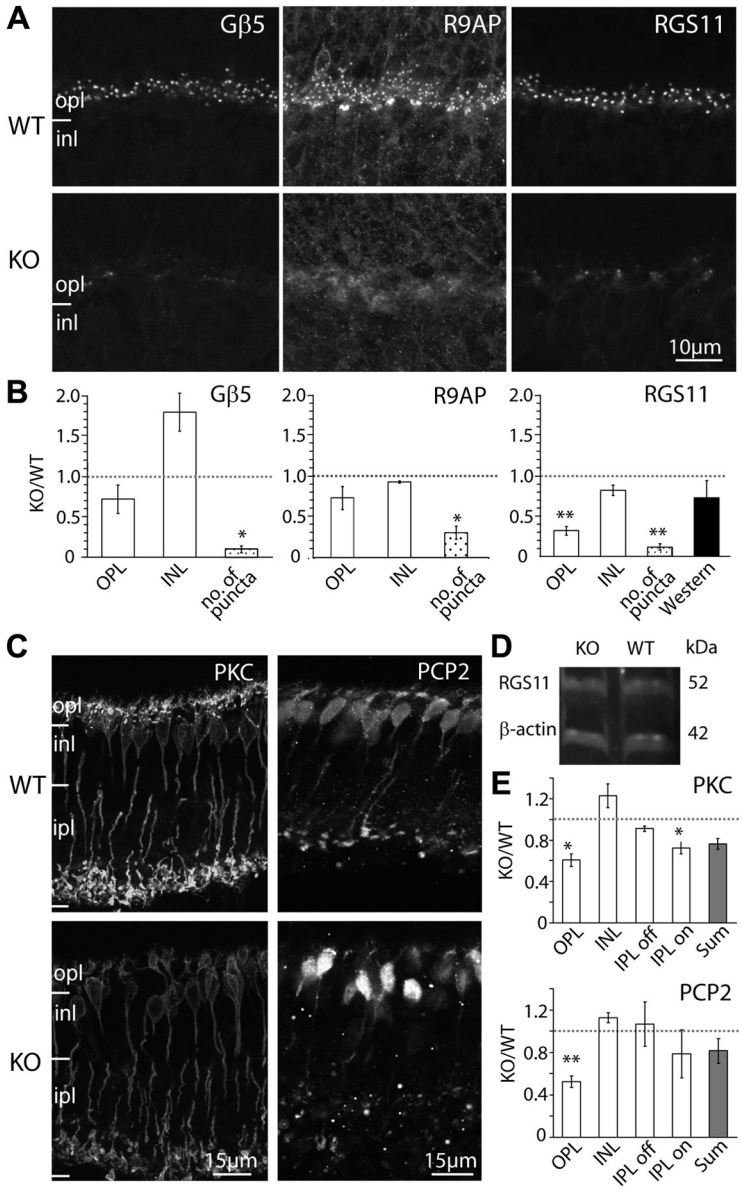

Figure 7. $G\beta_3$ deletion heavily affects modulators of the mGluR6 cascade that display a punctate appearance, but only mildly affects the diffusely distributed modulators. ***A***, Immunostaining of WT (top) and *Gnb3*-null (KO; bottom) mice for $G\beta_5$, R9AP, and RGS11. Punctate staining is greatly reduced in the null mouse. ***B***, Relative immunostaining (as defined in Fig. 6*C*) for these proteins in the outer plexiform and inner nuclear layers of the retina (white bars), relative puncta count (dotted bars), and band intensity from Western blots (for RGS11 only; dark bar). Punctate staining is greatly reduced in the null mouse. ***C***, Immunostaining of WT (top) and *Gnb3*-null (KO; bottom) mice for the diffuse modulators PKC and Ret-PCP2. ***D***, Western blot for RGS11 shows that the band intensity is similar between wild-type and *Gnb3*-null mice. ***E***, Relative immunostaining of various layers of the retina (white bars) and sum intensities of all layers (gray bars). $*p < 0.05$; $**p < 0.01$. Abbreviations are defined as in Figure 1.

number of profiles of rod terminals remained the same in wild-type and null mice (~200 in a section length of 200 μm), but the percentage of profiles containing at least one rod bipolar dendrite (the central element of the tetrad) decreased greatly from 43% in wild-type to 24% in null retina (three retinas per genotype) (Fig. 8*A–C*). The percentage of profiles that contained a ribbon (56% in wild-type vs 64% in null mice) and the percentage of profiles that contained one or more horizontal cell processes (62 vs 68%) did not decrease. We also examined cone terminals; these contained mitochondria and ribbons as in wild type, but some of these terminals appeared darker than in the wild type. The presynaptic membrane density appeared normal (Fig. 8*D*,*E*). However, since in rodents many of the contacts between the cone presynaptic membrane and the ON cone bipolar dendrite are made at the base of the cone similar to OFF bipolar cell contacts, reconstruction is necessary to count the ON bipolar cell dendrites (Vardi and Morigiwa, 1997).

To determine whether the deformed rod terminal results from a defect in development or maintenance, we examined the retina at 3 weeks of age, a time when development is almost complete (Olney, 1968; Blanks et al., 1974). Both wild-type and null retinas (two retinas per genotype) displayed percent profiles with ribbons and horizontal cell processes that were similar to older adults. However, in wild type, bipolar dendrites at 3 weeks of age were less frequent (37% at 3 weeks vs 43% in older adults) and appeared shorter than dendrites in older adults. Moreover, the presynaptic membrane was less dense than in the mature retina. These differences likely reflect incomplete development at this stage. In the null mouse, percentage profiles with a bipolar cell dendrite were only slightly reduced in the 3 week retina relative to the same age wild-type retina (33 vs 37%), and the 3 week null percentage was higher than that of older null mice (33 vs 24%) (Fig. 8*C*). Our results suggest that the developmental program is not affected in the null mouse, and thus the deficiency found in the adult is due to a failure to maintain the synaptic structure.

We also looked at the effect of age on the ERG wave. At 3 weeks in wild type, the a-wave was similar to that of older adults, but the rising phase of the b-wave appeared slower (implicit time to peak was 109 ms at 3 weeks and 90 ms at 4 weeks) (Fig. 8*F*), and the oscillatory potentials appeared slightly delayed (Fig. 8*G*). In contrast, at 3 weeks in the null mouse, the rising phase appeared faster than in older null adults and stayed at a higher relative value for ~100 ms, and the oscillatory potentials peaked at the same time (Fig. 8*H*,*I*) (albeit they peaked at a much later time than in wild type). This indicates that the residual response at 3 weeks is greater than it is at 4 weeks and older. This result is consistent with findings that the structure starts deteriorating within days after development is completed.

In mouse retina, $G\beta_3$ forms a complex with $G\alpha_o$

The absence of $G\beta_5$ or $G\beta_3$ leads to similar phenotypes, i.e., lack of ERG b-wave, mislocalization of RGS11 and R9AP, and reduction of intact triads. This raises the possibility that either $G\beta_3$ or $G\beta_5$ partners with $G\alpha_o$. We addressed this possibility by first examining the expression of the candidate G-protein subunits $G\alpha_o$, $G\beta_3$, and $G\gamma_{13}$ in the *Gnb5*-null retina. Staining for these proteins mimicked that in wild type (Fig. 9*A*,*B*). Moreover, localization of TRPM1 in this null retina was similar to that in wild

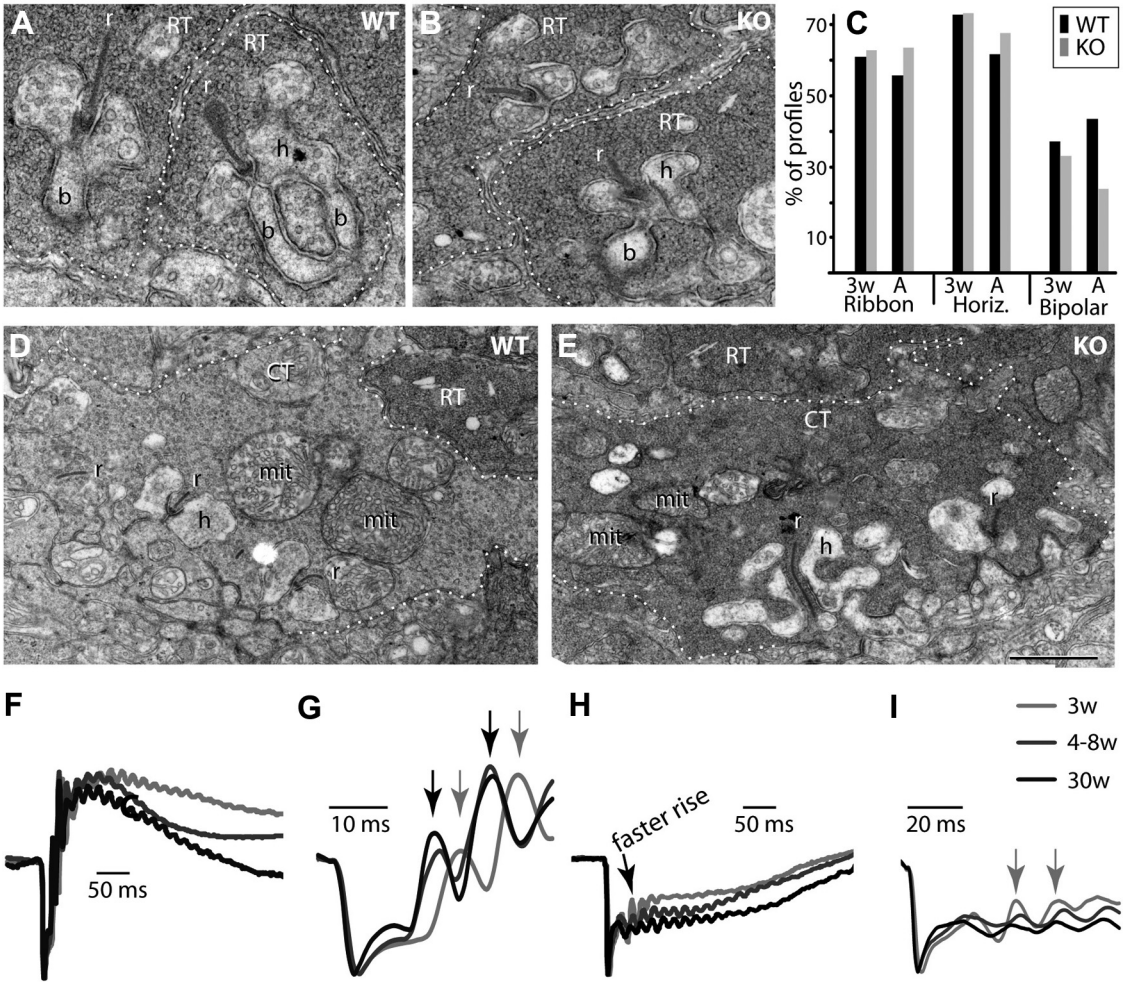

Figure 8. *Gnb3*-null rod bipolar dendrites are not maintained in the invagination of the rod terminal. ***A***, ***B***, Electron micrographs of rod terminals (RT). In WT retina, numerous profiles of rod terminals (outlined by dotted lines) are seen with one or two rod bipolar dendrites (b) postsynaptic to the rod's synaptic ribbon (r). In *Gnb3*-null (KO) retina, bipolar dendrites are usually smaller and are rarely observed. Horizontal cell processes (h) are seen with the same frequency in WT and KO. ***C***, Bar graph describes the percent of profiles in which a ribbon, at least one horizontal cell process (Horiz.), or at least one rod bipolar dendrite are observed. For each category, we show the percentage at 3 weeks (3w) and 4–7 weeks (A) for wild type (black) and *Gnb3* KO (gray). The number of profiles analyzed for WT were 218 (3w; $n = 2$) and 395 (A; $n = 3$), and for *Gnb3*-null they were 351 (3w; $n = 2$) and 404 (A; $n = 3$). The difference between WTs and nulls at 4–7 weeks was significant (χ^2 test, $p < 0.005$). ***D***, ***E***, Electron micrographs of cone terminals (CT). These terminals (outlined by dotted lines) are seen in both wild-type and null retinas, but in null retinas they appear darker with a density that resembles their neighboring rod terminals. mit, Mitochondrion. Scale bar: (in ***E***) ***A***, ***B***, 0.455 μm; ***D***, ***E***, 1 μm. ***F–I***, ERG records at different ages in wild-type (***F***, ***G***) and null (***H***, ***I***) mice. To compare shapes, we averaged traces from each age group and normalized this average trace to its minimum (peak of a-wave). The numbers of records averaged for each trace were 4 (3w), 6 (4–8w), and 2 (30w) for WT and 4 (3w), 6 (4–8w), and 4 (30w) for *Gnb3*-null. In ***G*** and ***I***, the time scale is expanded to show the initial oscillations. Note that in wild-type mice (***G***), the oscillations at 3 weeks lag behind those in older adults (gray and black arrows, respectively), while in null mice (***I***), they appear simultaneously (gray arrows), although they all lag behind the wild-type oscillations. Note the different time scales in ***G*** and ***I***.

type. Since the absence of $G\beta_5$ did not affect $G\alpha_o$ and $G\gamma_{13}$ expression, $G\beta_3$, but not $G\beta_5$, likely contributes to the G-protein heterotrimer. To further probe this issue, we performed coimmunoprecipitation using a mouse antibody against $G\alpha_o$ in the presence of GDPβS to pull down proteins that interact with inactive $G\alpha_o$. Probing the pulled down proteins was positive for $G\beta_3$ (three experiments) and negative for $G\beta_5$ (two experiments) (Fig. 9*C*,*D*). When anti-$G\alpha_o$ was omitted, $G\beta_3$ was not detected.

Discussion

We report here on two key discoveries. First, $G\beta_3$ is the partner of $G\alpha_o$ in the heterotrimer G-protein that switches on the mGluR6 cascade, yet it is not absolutely required for the light response since a small response can still be elicited in its absence. Second, $G\beta_3$ is required to maintain a healthy synapse, and its absence greatly affects expression of all proteins known to participate in the mGluR6 cascade.

Light responses in the absence of $G\beta_3$

mGluR6 clearly requires a heterotrimeric G-protein to couple it to the downstream cascade events that lead to closure of the TRPM1 channel (Nakajima et al., 1993). In ON bipolar cells, $G\alpha_{o1}$ is the main α subunit player (Dhingra et al., 2002), but $G\alpha_{o2}$ also provides a small response (Okawa et al., 2010). Here we identified $G\beta_3$ as the β subunit based on the following evidence: (1) Combined immunocytochemistry and/or examination of the ON bipolar cDNA library (data not shown) show that these cells express $G\beta_3$ and $G\beta_5$, but not $G\beta_1$, $G\beta_2$, and $G\beta_4$ (Lee et al., 1992; Peng et al., 1992). (2) Between these two expressed $G\beta$ subunits, the distribution of $G\beta_3$ within the cell most closely resembles that of $G\alpha_o$ and $G\gamma_{13}$; $G\gamma_{13}$ offers the best $G\gamma$ subunit candidate to form the $G\beta\gamma$ dimer in ON bipolar cells, and it has been shown to form functional dimers with $G\beta_3$ with high efficiency (Poon et al., 2009). (3) $G\beta_3$ deletion greatly reduces $G\gamma_{13}$ expression, while $G\beta_5$ deletion does not. (4) Coimmunoprecipitation of $G\alpha_o$ pulls

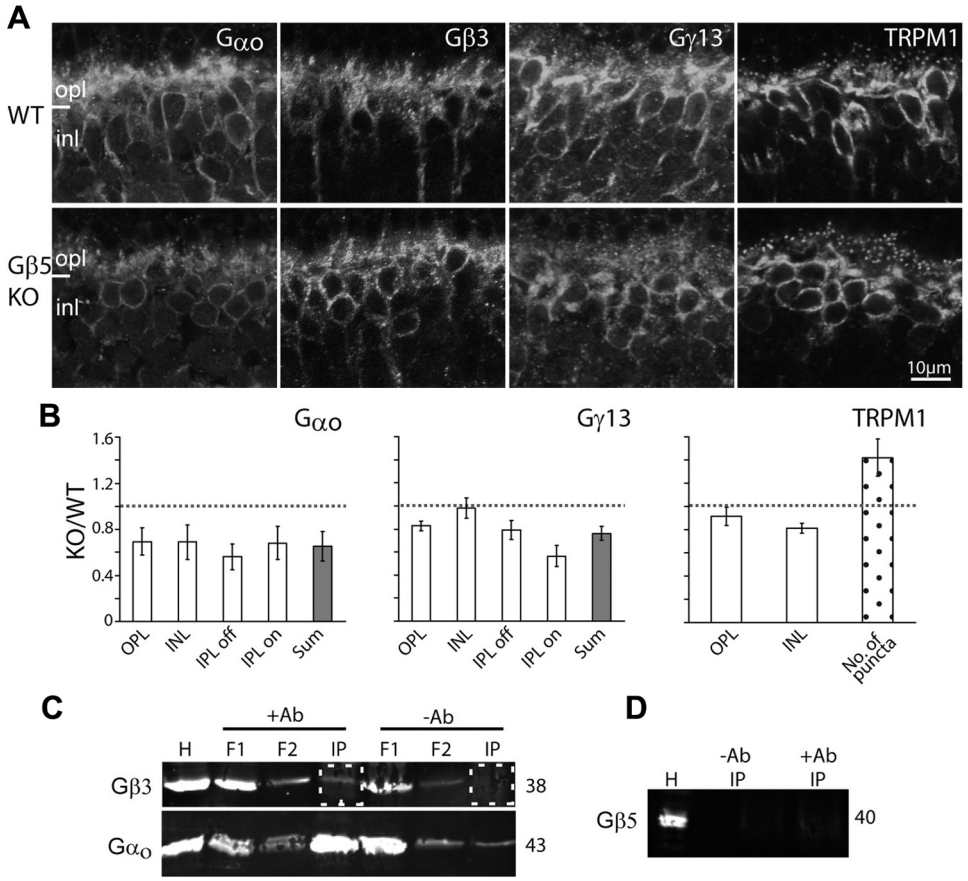

Figure 9. $G\beta_3$ rather than $G\beta_5$ forms the heterotrimer G_o. ***A***, Immunostaining in wild-type (top) and $G\beta_5$-null (bottom) retinas for $G\alpha_o$, $G\beta_3$, $G\gamma_{13}$, and TRPM1. Fixed retinas and sections were obtained from J. Chen. ***B***, Relative staining intensity (as defined in Fig. 6*C*) for $G\alpha_o$, $G\gamma_{13}$, and TRPM1 in several retinal layers and their sum. For TRPM1, the number of puncta was calculated as in previous figures. $G\beta_3$ staining was not quantified because staining only worked on one set of tissues. However, results from the Chen lab showed similar staining intensity in wild-type and null tissues (personal communications). Average ratios represent results from at least three sets of experiments. ***C***, Coimmunoprecipitation using a monoclonal antibody to pull down $G\alpha_o$ and its interacting proteins. The top blot was probed for $G\beta_3$, and bottom one for $G\alpha_o$. The relevant lanes, i.e., immunoprecipitated (IP) protein with and without the antibody, are boxed with dotted squares. H, Homogenate; F1, F2, flow through. ***D***, Coimmunoprecipitation samples probed for $G\beta_5$.

down $G\beta_3$, but not $G\beta_5$. Our conclusion that $G\beta_3$ partners with $G\alpha_o$ as a part of heterotrimer is consistent with knowledge that $G\beta_5$ is unique among $G\beta$ subunits, as in native tissues it interacts with members of R7 RGS family but not with $G\gamma$ subunits (Simonds and Zhang, 2000; Witherow et al., 2000) (for review, see Blake et al., 2001).

Since deletion of both splice variants of $G\alpha_o$ eliminates the light response (Dhingra et al., 2000; Okawa et al., 2010), it was expected that the heterotrimer is absolutely required. Thus, the residual light response that remained in the *Gnb3*-null retina was initially surprising. However, we now understand that if $G\beta_3$ elimination caused nothing else but a compromised G-protein complex, the residual light response would have been even greater. Indeed it appears that mechanisms exist that allow G-protein-coupled receptors to give significant responses without the complete native G-protein heterotrimer. In our study, the cone responds to a saturated light stimulus with a magnitude that is similar in null and wild-type mice (Dhingra et al., 2011). Similarly, in a mouse model where the rod $G\gamma_1$ was deleted, the rods showed a large response to saturating light stimuli as long as they were viable (Lobanova et al., 2008; Kolesnikov et al., 2011). Thus, these researchers concluded that although $G\gamma_1$ is required for efficient light responses, possibly to anchor $G\alpha_t$ and thereby increase the gain, the cascade can go forward without it, either by using a different $G\gamma$ or by a monomeric action of $G\alpha_t$. Similar explanations can be given for the ON bipolar cells. Regarding the possibility of using another $G\beta$, immunocytochemical staining for $G\beta_1$, $G\beta_2$, and $G\beta_4$ did not increase in null mice. It may be suggested that in the absence of $G\beta_3$, $G\beta_5$ binds $G\alpha_o$. However, we think this is unlikely because complexes of $G\beta_5$ with $G\alpha_o$ could not be detected in native tissues (present study) (Witherow et al., 2000) and because $G\beta_5$ is dramatically downregulated rather than upregulated in the *Gnb3*-null mouse. Nonetheless, it is possible that an undetectable amount of another $G\beta$ subunit is sufficient to support some response. As for the possibility that a monomeric $G\alpha$ can carry the cascade, it has been shown that $G\alpha_t$ can be activated by rhodopsin in the absence of $G\beta\gamma$, albeit inefficiently (Herrmann et al., 2006). If a monomeric action of $G\alpha_o$ is sufficient to close TRPM1 without the help of $G\beta\gamma$, it may indicate that, as with phototransduction and as suggested by Koike et al. (2010b), the $G\alpha$ subunit $G\alpha_o$, rather than the $G\beta\gamma$ dimer, carries the cascade forward to directly or indirectly close TRPM1. This interpretation, however, does not agree with recent interpretation that $G\beta\gamma$ carries the cascade (Shen et al., 2012).

Effect of $G\beta_3$ on synaptic proteins in the ON bipolar dendrite

We showed here that deletion of $G\beta_3$ from ON bipolar cells caused downregulation of $G\alpha_o$ and $G\gamma_{13}$, the G-protein subunits that likely form the heterotrimer. This is not surprising since these subunits are known to function as a heterotrimeric complex

in which the expression of one subunit typically affects that of the others. Moreover, these subunits associate together on the Golgi membrane before the heterotrimer is targeted to the plasma membrane (Michaelson et al., 2002). What is surprising is that the absence of Gβ_3 also produces downregulation of the receptor mGluR6 and the channel TRPM1. An even more dramatic effect was seen in the GAP complex that, in ON bipolar cells, is thought to comprise Gβ_5, R9AP, RGS7, and/or RGS11. The reduction of localized GAP complex that is observed in the *Gnb3*-null ON bipolar cells is similar to that seen in *Gnb5*-null, nob 4 (where a mutation in *Grm6* renders mGluR6 undetectable in the dendrite), and *Grm6*-null retinas (Cao et al., 2009; Xu et al., 2012). In *Gnb5*-null retina, downregulation or mislocalization of RGS7, RGS11, and R9AP is comparable to the downregulation of R9AP and RGS9 in photoreceptors of this null mouse, and thus was interpreted to indicate a tight GAP complex. Similarly, in the nob4 retina, reduction of the GAP complex was interpreted to mean that the complex requires mGluR6 for correct localization (Cao et al., 2009). Here, in the *Gnb3*-null retina, the GAP complex was severely affected while half of the mGluR6 was still correctly localized to the tips. Therefore, if mGluR6 is required for correct localization of the GAP complex, it is certainly not sufficient.

In further examining the localization of different cascade proteins in various null retinas, we noticed that the proteins of the GAP complex are greatly affected not only by the null mice mentioned above, but also in *Grm6*-null (Xu et al., 2012) and *Gnao* (Gα_o)-null (our unpublished data) retinas. This suggests that proteins of the GAP complex are dismantled more readily than the other cascade proteins. It has been shown in HEK cell expression systems that active Gα_o recruits Gβ_5/RGS7 dimer to the plasma membrane (Takida et al., 2005). This raises the possibility that reduced activity (due to the absence of cascade elements) translocates the GAP components out of the dendritic tips. Furthermore, this type of analysis suggests that certain proteins have independent instructions to traffic and concentrate at the dendritic tip, so their localization is not as affected by others. Possibly, the G-protein heterotrimer (or perhaps Gβ_3 itself) with its diffuse but gradient expression within the cell (i.e., strongest in the dendritic tips and weakest in the axon terminals) sets the stage for other cascade elements to traffic to the dendritic tips. This corresponds to the observation that Gβ_3 deletion causes a decline of almost every cascade or modulator element, but its own expression is not affected by deleting Gβ_5 or mGluR6 (Xu et al., 2012). To gain more insight into this issue, we are now examining the effects of deleting Gα_o in greater detail.

Effect of Gβ_3 on synaptic structure

Without Gβ_3, the majority of rod bipolar dendrites do not invaginate the rod terminal, and the characteristic central element of the synaptic tetrad was rarely observed. Failure to form a proper rod tetrad has also been shown in several mouse models with null or mutated synaptic proteins such as pikachurin, Gβ_5, mGluR6 (*nob 4* mouse), and RGS11+RGS7. In the pikachurin and Gβ_5 null retinas, the effect was due to a developmental defect (Rao et al., 2007; Sato et al., 2008; Shim et al., 2012). Interestingly, such a deficiency has not been described in the *Grm6*-null, Gα_o-null, or nyctalopin-null retinas (Pardue et al., 1998; Dhingra et al., 2000; Ball et al., 2003; Tsukamoto et al., 2007; Ishii et al., 2009).

We propose that proteins involved in the chemical organization of the rod-to-rod bipolar cell synapse are coregulated to form dynamic protein complexes, and many of them are restricted to the dendritic tips. For these dendritic tips to develop as invaginating dendrites and remain apposed to the rod membrane below the horizontal cell's invaginating processes, a chain of interacting proteins is required. We envision that Gβ_3 deletion mislocalizes mGluR6 and TRPM1, both are membrane proteins that interact with nyctalopin (Cao et al., 2011; Pearring et al., 2011), and this may affect expression of matrix proteins such as pikachurin. Thus, although the dendrite is likely developing by a genetic program to approach and invaginate the rod, the dendrite can only stabilize its relative position within the invagination when the presynaptic and postsynaptic complexes and the matrix proteins are in place to hold it there.

References

Ball SL, Pardue MT, McCall MA, Gregg RG, Peachey NS (2003) Immunohistochemical analysis of the outer plexiform layer in the nob mouse shows no abnormalities. Vis Neurosci 20:267–272.

Berrebi AS, Mugnaini E (1992) Characteristics of labeling of the cerebellar Purkinje neuron by L7 antiserum. J Chem Neuroanat 5:235–243.

Blake BL, Wing MR, Zhou JY, Lei Q, Hillmann JR, Behe CI, Morris RA, Harden TK, Bayliss DA, Miller RJ, Siderovski DP (2001) G beta association and effector interaction selectivities of the divergent G gamma subunit G gamma(13). J Biol Chem 276:49267–49274.

Blanks JC, Adinolfi AM, Lolley RN (1974) Synaptogenesis in the photoreceptor terminal of the mouse retina. J Comp Neurol 156:81–93.

Bomsel M, Mostov K (1992) Role of heterotrimeric G proteins in membrane traffic. Mol Biol Cell 3:1317–1328.

Cao Y, Masuho I, Okawa H, Xie K, Asami J, Kammermeier PJ, Maddox DM, Furukawa T, Inoue T, Sampath AP, Martemyanov KA (2009) Retina-specific GTPase accelerator RGS11/G beta 5S/R9AP is a constitutive heterotrimer selectively targeted to mGluR6 in ON-bipolar neurons. J Neurosci 29:9301–9313.

Cao Y, Posokhova E, Martemyanov KA (2011) TRPM1 forms complexes with nyctalopin in vivo and accumulates in postsynaptic compartment of ON-bipolar neurons in mGluR6-dependent manner. J Neurosci 31:11521–11526.

Chen CK, Burns ME, He W, Wensel TG, Baylor DA, Simon MI (2000) Slowed recovery of rod photoresponse in mice lacking the GTPase accelerating protein RGS9-1. Nature 403:557–560.

Chen FS, Shim H, Morhardt D, Dallman R, Krahn E, McWhinney L, Rao A, Gold SJ, Chen CK (2010) Functional redundancy of R7 RGS proteins in ON-bipolar cell dendrites. Invest Ophthalmol Vis Sci 51:686–693.

Dhingra A, Lyubarsky A, Jiang M, Pugh Jr EN, Birnbaumer L, Sterling P, Vardi N (2000) The light response of ON bipolar neurons requires Gα_o. J Neurosci 20:9053–9058.

Dhingra A, Jiang M, Wang TL, Lyubarsky A, Savchenko A, Bar-Yehuda T, Sterling P, Birnbaumer L, Vardi N (2002) Light response of retinal ON bipolar cells requires a specific splice variant of Gα_o. J Neurosci 22:4878–4884.

Dhingra A, Sulaiman P, Xu Y, Fina ME, Veh RW, Vardi N (2008) Probing neurochemical structure and function of retinal ON bipolar cells with a transgenic mouse. J Comp Neurol 510:484–496.

Dhingra A, Fina M, Nikonova E, Lyubarsky AL, Vardi N (2011) Cones function in the absence of Gβ3. Soc Neurosci Abstr 37:174.01.

Dupré DJ, Robitaille M, Rebois RV, Hébert TE (2009) The role of Gbetagamma subunits in the organization, assembly, and function of GPCR signaling complexes. Annu Rev Pharmacol Toxicol 49:31–56.

Grabowska D, Jayaraman M, Kaltenbronn KM, Sandiford SL, Wang Q, Jenkins S, Slepak VZ, Smith Y, Blumer KJ (2008) Postnatal induction and localization of R7BP, a membrane-anchoring protein for regulator of G protein signaling 7 family-Gbeta5 complexes in brain. Neuroscience 151:969–982.

Green DG, Kapousta-Bruneau NV (1999) A dissection of the electroretinogram from the isolated rat retina with microelectrodes and drugs. Vis Neurosci 16:727–741.

Herrmann R, Heck M, Henklein P, Hofmann KP, Ernst OP (2006) Signal transfer from GPCRs to G proteins: role of the G alpha N-terminal region in rhodopsin-transducin coupling. J Biol Chem 281:30234–30241.

Huang L, Max M, Margolskee RF, Su H, Masland RH, Euler T (2003) G protein subunit Ggamma13 is coexpressed with Galphao, Gbeta3 and Gbeta4 in retinal ON bipolar cells. J Comp Neurol 455:1–10.

Ishii M, Morigiwa K, Takao M, Nakanishi S, Fukuda Y, Mimura O, Tsuka-

moto Y (2009) Ectopic synaptic ribbons in dendrites of mouse retinal ON- and OFF-bipolar cells. Cell Tissue Res 338:355–375.

Jeffrey BG, Morgans CW, Puthussery T, Wensel TG, Burke NS, Brown RL, Duvoisin RM (2010) R9AP stabilizes RGS11-G beta5 and accelerates the early light response of ON-bipolar cells. Vis Neurosci 27:9–17.

Koike C, Numata T, Ueda H, Mori Y, Furukawa T (2010a) TRPM1: a vertebrate TRP channel responsible for retinal ON bipolar function. Cell Calcium 48:95–101.

Koike C, Obara T, Uriu Y, Numata T, Sanuki R, Miyata K, Koyasu T, Ueno S, Funabiki K, Tani A, Ueda H, Kondo M, Mori Y, Tachibana M, Furukawa T (2010b) TRPM1 is a component of the retinal ON bipolar cell transduction channel in the mGluR6 cascade. Proc Natl Acad Sci U S A 107:332–337.

Kolesnikov AV, Rikimaru L, Hennig AK, Lukasiewicz PD, Fliesler SJ, Govardovskii VI, Kefalov VJ, Kisselev OG (2011) G-protein betagamma-complex is crucial for efficient signal amplification in vision. J Neurosci 31:8067–8077.

Krispel CM, Chen CK, Simon MI, Burns ME (2003) Prolonged photoresponses and defective adaptation in rods of Gbeta5−/− mice. J Neurosci 23:6965–6971.

Lee RH, Lieberman BS, Yamane HK, Bok D, Fung BK (1992) A third form of the G protein beta subunit. 1. Immunochemical identification and localization to cone photoreceptors. J Biol Chem 267:24776–24781.

Lobanova ES, Finkelstein S, Herrmann R, Chen YM, Kessler C, Michaud NA, Trieu LH, Strissel KJ, Burns ME, Arshavsky VY (2008) Transducin gamma-subunit sets expression levels of alpha- and beta-subunits and is crucial for rod viability. J Neurosci 28:3510–3520.

Lyubarsky AL, Falsini B, Pennesi ME, Valentini P, Pugh EN Jr (1999) UV- and midwave-sensitive cone-driven retinal responses of the mouse: a possible phenotype for coexpression of cone photopigments. J Neurosci 19:442–455.

Lyubarsky AL, Daniele LL, Pugh EN Jr (2004) From candelas to photoisomerizations in the mouse eye by rhodopsin bleaching in situ and the light-rearing dependence of the major components of the mouse ERG. Vision Res 44:3235–3251.

Lyubarsky AL, Chen C, Simon MI, Pugh EN Jr (2000) Mice lacking G-protein receptor kinase 1 have profoundly slowed recovery of cone-driven retinal responses. J Neurosci 20:2209–2217.

Martemyanov KA, Arshavsky VY (2009) Biology and functions of the RGS9 isoforms. Prog Mol Biol Transl Sci 86:205–227.

Masu M, Iwakabe H, Tagawa Y, Miyoshi T, Yamashita M, Fukuda Y, Sasaki H, Hiroi K, Nakamura Y, Shigemoto R (1995) Specific deficit on the ON response in visual transmission by targeted disruption of the mGluR6 gene. Cell 80:757–765.

Masuho I, Celver J, Kovoor A, Martemyanov KA (2010) Membrane anchor R9AP potentiates GTPase-accelerating protein activity of RGS11 x Gbeta5 complex and accelerates inactivation of the mGluR6-G(o) signaling. J Biol Chem 285:4781–4787.

Michaelson D, Ahearn I, Bergo M, Young S, Philips M (2002) Membrane trafficking of heterotrimeric G proteins via the endoplasmic reticulum and Golgi. Mol Biol Cell 13:3294–3302.

Morgan JL, Dhingra A, Vardi N, Wong RO (2006) Axons and dendrites originate from neuroepithelial-like processes of retinal bipolar cells. Nat Neurosci 9:85–92.

Morgans CW, Wensel TG, Brown RL, Perez-Leon JA, Bearnot B, Duvoisin RM (2007) Gbeta5-RGS complexes co-localize with mGluR6 in retinal ON-bipolar cells. Eur J Neurosci 26:2899–2905.

Morgans CW, Brown RL, Duvoisin RM (2010) TRPM1: the endpoint of the mGluR6 signal transduction cascade in retinal ON-bipolar cells. Bioessays 32:609–614.

Nakajima Y, Iwakabe H, Akazawa C, Nawa H, Shigemoto R, Mizuno N, Nakanishi S (1993) Molecular characterization of a novel retinal metabotropic glutamate receptor mGluR6 with a high agonist selectivity for L-2-amino-4-phosphonobutyrate. J Biol Chem 268:11868–11873.

Ng L, Lyubarsky A, Nikonov SS, Ma M, Srinivas M, Kefas B, St Germain DL, Hernandez A, Pugh EN Jr, Forrest D (2010) Type 3 deiodinase, a thyroid-hormone-inactivating enzyme, controls survival and maturation of cone photoreceptors. J Neurosci 30:3347–3357.

Okawa H, Pahlberg J, Rieke F, Birnbaumer L, Sampath AP (2010) Coordinated control of sensitivity by two splice variants of Galpha(o) in retinal ON bipolar cells. J Gen Physiol 136:443–454.

Olney JW (1968) An electron microscopic study of synapse formation, receptor outer segment development, and other aspects of developing mouse retina. Invest Ophthalmol 7:250–268.

Pardue MT, McCall MA, LaVail MM, Gregg RG, Peachey NS (1998) A naturally occurring mouse model of X-linked congenital stationary night blindness. Invest Ophthalmol Vis Sci 39:2443–2449.

Pearring JN, Bojang P Jr, Shen Y, Koike C, Furukawa T, Nawy S, Gregg RG (2011) A role for nyctalopin, a small leucine-rich repeat protein, in localizing the TRP melastatin 1 channel to retinal depolarizing bipolar cell dendrites. J Neurosci 31:10060–10066.

Peng YW, Robishaw JD, Levine MA, Yau KW (1992) Retinal rods and cones have distinct G protein beta and gamma subunits. Proc Natl Acad Sci U S A 89:10882–10886.

Poon LS, Chan AS, Wong YH (2009) Gbeta3 forms distinct dimers with specific Ggamma subunits and preferentially activates the beta3 isoform of phospholipase C. Cell Signal 21:737–744.

Rao A, Dallman R, Henderson S, Chen CK (2007) Gbeta5 is required for normal light responses and morphology of retinal ON-bipolar cells. J Neurosci 27:14199–14204.

Ritchey ER, Bongini RE, Code KA, Zelinka C, Petersen-Jones S, Fischer AJ (2010) The pattern of expression of guanine nucleotide-binding protein beta3 in the retina is conserved across vertebrate species. Neuroscience 169:1376–1391.

Robson JG, Frishman LJ (1995) Response linearity and kinetics of the cat retina: the bipolar cell component of the dark-adapted electroretinogram. Vis Neurosci 12:837–850.

Sato S, Omori Y, Katoh K, Kondo M, Kanagawa M, Miyata K, Funabiki K, Koyasu T, Kajimura N, Miyoshi T, Sawai H, Kobayashi K, Tani A, Toda T, Usukura J, Tano Y, Fujikado T, Furukawa T (2008) Pikachurin, a dystroglycan ligand, is essential for photoreceptor ribbon synapse formation. Nat Neurosci 11:923–931.

Shen Y, Rampino MA, Carroll RC, Nawy S (2012) G-protein-mediated inhibition of the Trp channel TRPM1 requires the Gbetagamma dimer. Proc Natl Acad Sci U S A 109:8752–8757.

Shim H, Wang CT, Chen YL, Chau VQ, Fu KG, Yang J, McQuiston AR, Fisher RA, Chen CK (2012) Defective retinal depolarizing bipolar cells (DBCs) in Regulators of G-protein Signaling (RGS) 7 and 11 double null mice. J Biol Chem 287:14873–14879.

Simonds WF, Zhang JH (2000) New dimensions in G protein signalling: G beta 5 and the RGS proteins. Pharm Acta Helv 74:333–336.

Takida S, Fischer CC, Wedegaertner PB (2005) Palmitoylation and plasma membrane targeting of RGS7 are promoted by alpha o. Mol Pharmacol 67:132–139.

Tsukamoto Y, Morigiwa K, Ishii M, Takao M, Iwatsuki K, Nakanishi S, Fukuda Y (2007) A novel connection between rods and ON cone bipolar cells revealed by ectopic metabotropic glutamate receptor 7 (mGluR7) in mGluR6-deficient mouse retinas. J Neurosci 27:6261–6267.

Vardi N, Morigiwa K (1997) ON cone bipolar cells in rat express the metabotropic receptor mGluR6. Vis Neurosci 14:789–794.

Vardi N, Matesic DF, Manning DR, Liebman PA, Sterling P (1993) Identification of a G-protein in depolarizing rod bipolar cells. Vis Neurosci 10:473–478.

Weinstein LS, Chen M, Xie T, Liu J (2006) Genetic diseases associated with heterotrimeric G proteins. Trends Pharmacol Sci 27:260–266.

Witherow DS, Wang Q, Levay K, Cabrera JL, Chen J, Willars GB, Slepak VZ (2000) Complexes of the G protein subunit gbeta 5 with the regulators of G protein signaling RGS7 and RGS9. Characterization in native tissues and in transfected cells. J Biol Chem 275:24872–24880.

Xu Y, Sulaiman P, Feddersen RM, Liu J, Smith RG, Vardi N (2008) Retinal ON bipolar cells express a new PCP2 splice variant that accelerates the light response. J Neurosci 28:8873–8884.

Xu Y, Dhingra A, Fina ME, Koike C, Furukawa T, Vardi N (2012) mGluR6 deletion renders the TRPM1 channel in retina inactive. J Neurophysiol 107:948–957.

Zhang J, Jeffrey BG, Morgans CW, Burke NS, Haley TL, Duvoisin RM, Brown RL (2010) RGS7 and -11 complexes accelerate the ON-bipolar cell light response. Invest Ophthalmol Vis Sci 51:1121–1129.